



HAL
open science

Reaction pathways, kinetics and toxicity assessment during the photocatalytic degradation of glyphosate and myclobutanil pesticides: Influence of the aqueous matrix

Patricia Garcia-Muñoz, Werner Dachtler, Bernd Altmayer, Ralf Schulz, Didier Robert, Frank Seitz, Ricki Rosenfeldt, Nicolas Keller

► To cite this version:

Patricia Garcia-Muñoz, Werner Dachtler, Bernd Altmayer, Ralf Schulz, Didier Robert, et al.. Reaction pathways, kinetics and toxicity assessment during the photocatalytic degradation of glyphosate and myclobutanil pesticides: Influence of the aqueous matrix. *Chemical Engineering Journal*, 2019, pp.123315. 10.1016/j.cej.2019.123315 . hal-02354789

HAL Id: hal-02354789

<https://hal.science/hal-02354789>

Submitted on 15 Dec 2020

HAL is a multi-disciplinary open access archive for the deposit and dissemination of scientific research documents, whether they are published or not. The documents may come from teaching and research institutions in France or abroad, or from public or private research centers.

L'archive ouverte pluridisciplinaire **HAL**, est destinée au dépôt et à la diffusion de documents scientifiques de niveau recherche, publiés ou non, émanant des établissements d'enseignement et de recherche français ou étrangers, des laboratoires publics ou privés.

1 **Reaction pathways, kinetics and toxicity assessment during**
2 **the photocatalytic degradation of glyphosate and**
3 **myclobutanil pesticides: Influence of the aqueous matrix.**

4 **Patricia Garcia-Muñoz,^{1,*} Werner Dachtler,² Bernd Altmayer,² Ralf Schulz,³ Didier Robert,¹**
5 **Frank Seitz,^{3,4} Ricki Rosenfeldt,^{3,4} and Nicolas Keller^{1,*}**

6
7 1 Institut de Chimie et Procédés pour l’Energie, l’Environnement et la Santé (ICPEES),
8 CNRS/University of Strasbourg, 25 rue Becquerel, Strasbourg, France

9 2 Dienstleistungszentrum Ländlicher Raum (DLR) Rheinpfalz, Institute of Plant Protection,
10 Breitenweg 71, Neustadt an der Weinstraße, Germany

11 3 Institute for Environmental Sciences, University of Koblenz-Landau, Campus Landau,
12 Fortstrasse 7, 76829 Landau, Germany

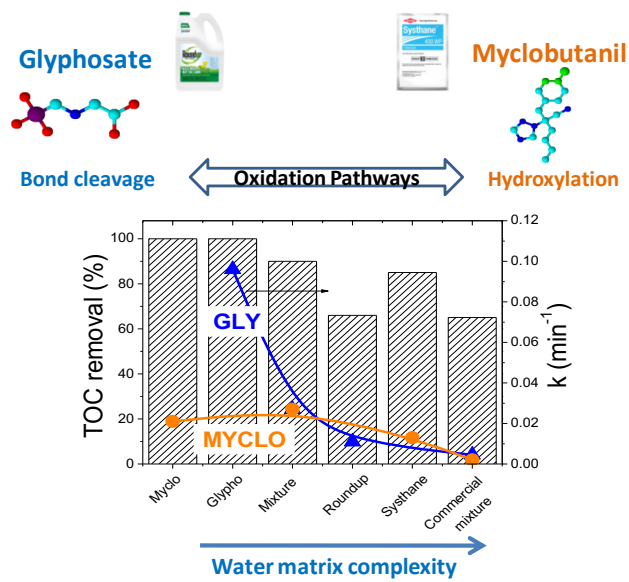
13 4 nEcoTox, An der Neumühle 2, Annweiler, Germany

14
15 * corresponding authors: Patricia Garcia-Muñoz : garciamunoz@unistra.fr – Nicolas Keller :
16 nkeller@unistra.fr

21

GRAPHICAL ABSTRACT

22



23

24

25

26 **ABSTRACT**

27 Assessment of reaction pathways, kinetics and water toxicity during the photocatalytic degradation
28 of glyphosate and myclobutanil pesticides has been performed in different aqueous matrices of
29 increasing complexity, from the single pesticides to the mix of their commercial formulations. Using
30 Aeroxide®-TiO₂-P25 as reference UV-A (Ultraviolet A) light photocatalyst, the ability of photocatalysis
31 to degrade glyphosate and myclobutanil pesticides in water was evidenced independently of the
32 aqueous matrix complexity, complete mineralization into CO₂, phosphate and chloride ions being
33 achieved. Further, an unusual volcano-like TOC evolution profile resulting from the proposed
34 glyphosate degradation pathway was observed whatever the aqueous matrix. Increasing the water
35 matrix complexity from single pesticides to the commercial formulation mix reduced the degradation
36 kinetics and consequently extended the time necessary for complete mineralization but, did not
37 influence the overall pesticide fate profiles. This behavior was associated to the competitive
38 adsorption of the organic matter onto the catalyst and to the presence of ions and inorganic matter.
39 The co-presence of glyphosate and to lesser extent of Roundup® formulation additives strongly
40 impacted the myclobutanil fate profile, due to preferential adsorption/degradation of glyphosate. By
41 contrast, despite their impact on the degradation pathway, the inorganic additives of the Systhane®
42 formulation influenced to a lesser extent both myclobutanil removal duration and TOC removal
43 compared to glyphosate/Roundup® products. The treatment allowed for most of the cases a strong
44 reduction of acute toxicity to aquatic invertebrate test organisms (*D.magna*) whatever the water
45 matrix complexity, while the ecotoxicity was reduced by half for the complex formulation mix.

46

47 **KEYWORDS:** photocatalysis, glyphosate, myclobutanil, oxidation pathway, wastewater matrix effect

48

49

50 1. INTRODUCTION

51

52 Synthetic pesticides have been intensively used worldwide since half a century for protecting
53 crops. In the center of Europe, particularly in the surroundings of the Upper Rhine river, viticulture
54 remained one of the crops most subjected to pesticide treatments for protecting from local pests
55 and consequently maintaining exploitation yields. Within this area, the main fungicide treatments
56 applied generate 70% of the total grapevine growing costs [1]. For instance, French vineyards
57 represent 30% of the overall pesticide use, while they account for only 3% of all farmland.
58 Unfortunately, while their use allowed a strong increase in the crop yields and the development of
59 intensive farming, their appearance in freshwater bodies and soils negatively affects the
60 environment and the human health. One important sources of these compounds for the natural
61 water bodies is the washing water arising from the cleaning of agricultural spraying machineries
62 following application.

63 While wastewater effluents should therefore be treated prior to discharge, conventional
64 treatments based on mechanical, physical, chemical or biological processes are facing with the
65 increase in the volume and the load of the pollutants in these effluents, the reduction of the
66 biodegradability of the pollutants, as well as with the heterogeneity of the water matrix [2-4]. Among
67 the Advanced Oxidation Processes (AOPs) that are emerging as feasible alternatives or complements
68 to conventional wastewater treatment plants for treating waters contaminated by refractory
69 compounds [5], photocatalysis has gained important attention due to a high efficiency and relatively
70 low costs, when working with low charges of pollutant, as well as to its ability to degrade the
71 biorecalcitrant and emerging contaminants [6, 7]. It allows achieving a complete mineralization of
72 refractory substrates thanks to its ability to oxidize short-chain acids and enables operating
73 efficiently in an extended working pH range, while taking advantage of a versatile and
74 environmentally-friendly implementation [5].

75 Although intense efforts have been made to enhance the degradation rate of pesticides and
76 more generally the mineralization yields of photocatalytic processes, TiO₂ still remains the
77 photocatalyst *par excellence* provided that a UV-A (Ultraviolet A) light irradiation is targeted, so that
78 it has been employed in the photodegradation of a large variety of pesticides in the last decades [1,
79 8-11]. The process time necessary for removing and mineralizing pesticides from water and
80 consequently for reducing the associated toxicity is known to strongly differ depending on the active
81 substance, since both composition and chemical structure of the target pesticide impact on the
82 degradation pathways and the reaction intermediates [9, 12]. Furthermore, pesticides often occur as
83 mixtures in surface waters, and they are always applied as commercial formulations containing
84 various kinds of organic and/or inorganic additives in addition to the active substance. Therefore, the
85 ability of photocatalysis for treating water containing pesticide mixtures [10, 11] and commercial
86 pesticide formulations [1, 13], as well as the influence of the water matrix complexity, *eg.* the
87 amount and composition of extra-load [14], on the pesticide degradation process and more generally
88 on the efficiency of the water treatment, are highly worth being investigated.

89 The herbicide *glyphosate* and the fungicide *myclobutanil* are two fundamentally different
90 compounds among the pesticides that are most frequently detected in the Upper Rhine river area
91 [15], glyphosate being a P- and N- containing aliphatic substrate, while myclobutanil is a N- and Cl-
92 containing substrate with both C-C and N-C aromatic rings and aliphatic branch. Used as the
93 commercial formulations Roundup® and Systhane®, respectively, they appeared at relatively high
94 concentrations in wastewater because of their prolonged use. Glyphosate (C₃H₈NO₅P) is a broad
95 spectrum organophosphate systemic herbicide that has shown resistance to natural degradation
96 pathways due to its inert C-P bond. Recent studies have demonstrated that glyphosate has negative
97 effects on ecosystems and humans. It provokes severe effects to many non-targeted organisms, with
98 for instance effects on reproduction in soil invertebrates, changes in the zooplankton behavior,
99 reduction of fertility in some fishes [16, 17]. Furthermore, anxiety and depression have been
100 observed for mice following chronic exposure. Detected in surface and groundwater, myclobutanil

101 (C₁₅H₁₇ClN₄) is a triazole pesticide used to avoid fungi infection, the main environmental risk of which
102 being related to the potential formation of bioactive (toxic) metabolites [18]. Moreover, fungicides
103 are generally known to be capable of causing endocrine activities [19] and chronic effects [20] even
104 at low concentrations of 3 µg/L. It has to be mentioned that no direct and straightforward
105 relationship is established between the Total Organic Carbon (TOC) depletion and the toxicity
106 reduction of an effluent [21-23], mainly due to formation of potentially-harmful reaction
107 intermediates, to the presence in the commercial formulations of non-inert inorganic additives, as
108 well as to synergistic interaction effects between the aqueous substances along the treatment. For
109 instance, Kohler et al. obtained 80% of TOC reduction with simultaneously an important increase in
110 the toxicity [21], while Supowit et al. treated fipronil-contaminated water and indicated that the
111 generation of harmful intermediates provoked a rise in toxicity values [23]. Therefore, the toxicity
112 assessment of the effluent has to be performed along the process simultaneously to the
113 determination of the reaction kinetics and of the TOC removal efficiency.

114 The ability of photocatalysis to degrade both glyphosate [24-27] and myclobutanil [27, 28]
115 pesticides has already been demonstrated. Therefore, the novelty of this work is to study their
116 photocatalytic degradation in different aqueous matrices of increasing complexity, from the single
117 pesticides to the mix of their Roundup® and Systhane® commercially available formulations, and to
118 assess the reaction pathways that take place in different matrices, the kinetics and the water
119 ecotoxicity during the treatment. We highlighted that, in addition to its influence on the reaction
120 kinetics, the aqueous matrix complexity strongly impacted on the reaction pathways followed for
121 reaching the mineralization of the substrates. To this end, the study has been performed using the
122 well-known commercial Aeroxide® TiO₂-P25, considered *de facto* as the reference photocatalyst
123 under UV-A light, as a first step necessary for shedding light on the influence of the aqueous matrix
124 complexity on the water treatment efficiency during the degradation of glyphosate and myclobutanil
125 pesticides.

126

127 **2- MATERIALS AND METHODS**

128

129 **2.1 Materials and formulations**

130 Analytical grade reagents were used without any further purification. Glyphosate (N-
131 (phosphonomethyl)glycine, >99%) and Myclobutanil ((RS)-2-p-chlorophényl-2-(1H-1,2,4-triazole-1-
132 ylméthyl)hexanenitrile, >99%) were purchased from HPC *High Purity Compounds* (Cunnersdorf,
133 Germany).

134 Roundup®-720 and Systhane®-200 products were commercially available formulations from
135 Monsanto and Dow agrosiences, containing 720 g/L glyphosate and 200 g/L myclobutanil pesticides
136 as active compounds, respectively. Table 1 and Table 2 show the composition expressed in mass
137 percentage of the Roundup® and Systhane® products and the main physico-chemical parameters of
138 the ready-to-use diluted formulations. Roundup® and Systhane® formulations displayed very distinct
139 compositions. Beside the presence of their respective active compound, in both formulations with a
140 *ca.* 40 wt.% fraction, Roundup® has been reported to contain additional carbon-containing molecules
141 such as isopropylamine and surfactants, whereas by contrast Systhane® was characterized by the
142 presence of several oxides and salts. Therefore, as a result of the diversity of the carbon sources
143 within the Roundup® formulation, the glyphosate active compound amounted only for a fraction of
144 the total TOC recorded for the commercial formulation, while in the case of the Systhane®
145 formulation, the TOC only resulted from the myclobutanil itself. Both Roundup® and Systhane®
146 solutions were prepared with a concentration of the active compound similar to that of the synthetic
147 pesticide mixed solution, *i.e.* at 25 mg/L and 35 mg/L, respectively. We have to stress that the highly
148 viscous nature of the commercial Systhane® paste somehow jeopardizes the initial myclobutanil
149 concentration in the case of the degradation tests with the commercial products. This has been
150 specified where appropriate.

151 Commercial Aeroxide® TiO₂-P25 was obtained from Evonik. The isoelectrical point of the

152 TiO₂-P25 powder has been measured at 6.3 by zeta potential measurement.

153

154 **2.2 Typical reaction procedure**

155 Experiments were carried out in a batch beaker-type glass reactor at atmospheric pressure,
156 room temperature (20 °C) and using O₂ from the atmosphere as oxidant, air being pumped into the
157 reactor at 150 mL/min for preventing from any oxygen deficiency into the reaction media. The
158 reactor was placed in a thermostated chamber for maintaining a constant temperature during the
159 tests. The photocatalytic tests have been performed under stirring at 600 rpm with a reaction
160 volume of 250 mL at a 1 g/L Aeroxide® TiO₂-P25 catalyst load. Independently of the aqueous matrix
161 complexity, stirring the suspension for 0.5 h in the dark enabled the establishment of the dark
162 adsorption/desorption equilibrium before turning on the irradiation (Figure S1). The suspension was
163 further exposed to a 60 W/m² irradiance UV-A light centered at 365 nm, provided by Philips
164 24W/10/4P lamps. At each time interval, the solution has been sampled and further filtered through
165 0.20 µm porosity filter for removing the photocatalyst powder, before being analyzed. All glyphosate
166 and myclobutanil degradation experiments have been triplicated, with standard deviation remaining
167 within the ±3% relative range, so that no standard error bars have been reported on the graphs for
168 sake of clarity.

169 Regardless of the water matrix, neither glyphosate or myclobutanil degradation, nor TOC
170 reduction has been observed in the absence of the photocatalyst. This indicated that the photolysis
171 of the pesticides or of the carbonated additives in the commercial formulations can be neglected under
172 UV-A in the experimental conditions.

173

174 **2.3 Analysis techniques**

175 The analysis of glyphosate and of both aminomethylphosphonic acid (AMPA) and primary
176 amine (sarcosine) intermediates was performed by mass spectrometry with an Agilent 1260 Infinity

177 HPLC Quadrupole Time of Flight Mass Spectrometer 6530A. Myclobutanil was analyzed by UV-Visible
178 spectrophotometry (Cary-100 Scan Varian Inc.) by following the disappearance of the main
179 absorption peak at $\lambda = 220$ nm as reaction samples were withdrawn from the reaction medium, while
180 the analysis of the main high carbon number reaction intermediates was performed by mass
181 spectrometry with an Agilent 1260 Infinity HPLC Quadrupole Time of Flight Mass Spectrometer
182 6530A. A typical chromatogram obtained during the photocatalytic treatment of a solution
183 containing glyphosate and myclobutanil pesticides can be seen in Figure S2. Anions and cations as
184 well as the short-chain acids were analyzed by ion chromatography (Metrohm 790IC) using a
185 conductivity detector. A Metrosep A supp 5–250 column (25 cm length, 4 mm diameter) was
186 employed as stationary phase, while an aqueous solution containing 3.2 mM Na_2CO_3 and 1 mM
187 NaHCO_3 was employed as mobile phase at a flow rate of 1 mL min^{-1} . Total Organic Carbon (TOC)
188 measurements were performed using a TOC analyzer (Shimadzu, model TOC-L) for determining the
189 organic carbon load.

190

191 **2.4 Ecotoxicological tests**

192 The ecotoxicity of the aqueous pesticide solutions (untreated and after photocatalytic
193 treatments) was addressed after filtration by performing 48 h acute toxicity tests with *Daphnia*
194 *magna* according to the OECD guideline 202 (2004) [29]. In the following, the aqueous pesticide
195 solutions will be named test items. Prior each test, the test item was serially diluted in the test
196 medium (daphnia culturing water (ASTM-medium [29])). The highest possible concentration was 50%
197 test item and 50% test medium, since the daphnids do not survive in deionized water.

198 Briefly, juveniles (age < 24 h) were exposed in groups of five organisms (n=4) to the dilution
199 series of the test item in the test medium. At the end of each test, immobile organisms were counted
200 and if applicable the EC_{50} value (*ie.* the test item concentration (in %) at which 50% of the daphnids
201 were immobilized) was calculated for each test item by applying a dose-response modeling. Thereby

202 the EC₅₀ values were expressed as percent of test item (% v/v) within the total test solution (= %TI).
203 So, the lower the %TI, the higher is the toxicity. This enables a direct comparison of the toxicity
204 before and after photocatalytic treatment without having the information about i) the exact
205 concentration of the active ingredient and ii) further implications such as *eg.* the impact of additional
206 formulation ingredients.

207 However, the toxicity outcomes (= 48 h-EC₅₀ values (%)) were statistically compared using
208 confidence interval testing to unravel a potential change of toxicity during the photocatalytic
209 treatment of the pesticide-containing solutions.

210

211 **3- RESULTS AND DISCUSSION**

212

213 **3.1 Degradation of single pesticides**

214 **3.1.1. Degradation of glyphosate**

215 Figure 1 shows the evolution with time under irradiation of both the glyphosate removal and the
216 phosphate release in %, of the TOC and of the pH value. The evolution of the concentration of the
217 short-chain acids, of both nitrate and ammonium ions, and of the aminomethylphosphonic acid
218 (AMPA) intermediate has been also reported. A high adsorption of glyphosate onto the TiO₂ surface
219 has been observed during the adsorption/desorption equilibrium period in the dark ($\approx 50\%$), that was
220 accompanied with a notable rise in pH from 4.2 to 6. This resulted from the favoured interaction at
221 the initial acidic pH of the negatively-charged glyphosate ($pK_a=0.8$) with the positively-charged titania
222 surface. After the adsorption/desorption equilibrium has been reached, a complete glyphosate
223 depletion has been observed within the first 30 min of reaction. By contrast, an unusual volcano-like
224 profile was observed for the TOC evolution during the course of the photocatalytic process, that
225 exhibited a maximum at t_{60} before the complete mineralization of glyphosate was achieved at t_{240} . It
226 was worth noting that this initial increase of TOC was occurring together with the glyphosate

227 disappearance, the simultaneous release of phosphates that closed the phosphorous balance and
228 the detection of reaction intermediates such as AMPA and acetic acid. This suggested that the
229 initially produced radicals were employed preferentially for cleaving bonds such as P-C or N-C rather
230 than C-C bonds, since no reduction of the overall carbon content was observed at the beginning of
231 the process. So, the increase in TOC observed for 60 min was proposed to be due to the desorption
232 of the first reaction intermediates resulting from the P-C and N-C bond cleavage. Following the
233 cleavage of these bonds to yield lower molecular weight compounds, typical oxidation steps took
234 place, provoking the appearance of other short-chain acids (formic and oxalic acids) as a
235 consequence of a classical oxidation route, and leading to the total mineralization of the initial
236 compound after 240 min (Figure 1) [30-32]. This was in agreement with the pH evolution profile
237 during the test, with an initial drop at the beginning of the test, and a subsequent increase back to 6,
238 as a result from the oxidation of the short-chain organic acid intermediates and potentially from the
239 formation of ammonia.

240 The glyphosate degradation has been suggested to occur through two different pathways
241 (Figure 2), both involving the breakdown of the glyphosate molecule into smaller compounds with no
242 reduction of the overall carbon content. The first pathway may consist in the hydroxylation of the
243 electrophilic N-C bond, that led to the formation of AMPA (aminomethylphosphonic acid, one of the
244 most frequently detected degradation intermediates of glyphosate in natural water bodies) and to
245 acetic acid (Figure 2A-right), in agreement with Assalin et al. [24]. Please note that the AMPA
246 pathway may bypass acetic acid and form glyoxalic acid directly, as proposed by Jaisi et al. [33]. In
247 the second pathway, the attack of the P-C bond by the oxidizing radicals ($\text{HO}\bullet$ or $\text{O}_2\bullet^-$) would result
248 in the cleavage of the molecule with the direct release of phosphate to water and the formation of
249 the sarcosine (2- (Methylamino)acetic acid) intermediate (Figure 2A-left). The formation of sarcosine
250 was reported notably by Jaisi et al. [33] and Echavia et al. [26]. The carbon-containing compounds
251 suffered from further degradation yielding the corresponding aliphatic structures (Figure 2B),

252 subsequently completely mineralized into their corresponding ions and CO₂ (Figure 2C). The
253 proposed degradation route was in agreement with previous studies [26].

254 Initially, the glyphosate solution showed no toxicity for daphnids (EC₅₀ > 50 %TI; Table 3),
255 since the initial glyphosate concentration of 25 mg/L was below the 48 h-EC₅₀ for aquatic
256 invertebrates (40 mg glyphosate/L) according to the toxicity information from the Pesticide
257 Properties Data Base. However, a moderate increase in toxicity was observed for the sample treated
258 for 120 min with an EC₅₀ value of 41 %TI, before the solution exhibited again subsequently no toxicity
259 after 240 min of treatment (no 48h-EC₅₀ determinable), in good agreement with the complete
260 oxidation of the different intermediate compounds (Figure 1). This toxicity profile could be ascribed
261 to the formation of potentially toxic reaction intermediates.

262

263 **3.1.2. Degradation of myclobutanil**

264 Figure 3A shows the evolution with time under irradiation of the myclobutanil removal rate
265 in %, of the TOC and of the pH value, while that of the concentration of short-chain acids as well as of
266 both nitrate and ammonium ions is shown in Figure 3B, together with that of the chloride release in
267 %. First, the establishment of the adsorption/desorption equilibrium in the dark evidenced a removal
268 of 20% of myclobutanil (pK_a=2.3). Myclobutanil was subsequently removed within 150 min of
269 reaction while the TOC evolution displayed a usual decreasing profile since the beginning of the
270 reaction for reaching a complete mineralization within 240 min of reaction. The complete
271 mineralization was confirmed by the presence of short chain acids during the reaction, intermediates
272 generated at the latest oxidation stages, as well as by the complete closure of the chloride balance
273 by chloride ions at 240 min, that evidenced the absence of any residual organochloride species at the
274 end of the reaction. No formation of chlorinated short-chain organic acids was observed throughout
275 the test.

276 While other authors have reported that the chloride elimination was the first step in the
277 oxidation of aromatic substrates [34, 35], in the present study the chloride release was only observed
278 after 60 min of reaction. A similar delayed chloride release was observed by Lai et al. [36] during the
279 photodegradation of oxazaphosphorine with titania. Figure 4 shows the reaction intermediates and
280 the final products detected during the photocatalytic degradation of myclobutanil, and Figure S3-A
281 shows the intensity profile of the main aromatic intermediates detected by HPLC/MS, that displayed
282 the typical profile for sequential reactions with intermediate compounds. First, the formation of C₁₅-
283 Cl and C₁₀-Cl organochloride intermediates during the reaction corroborated the late release of
284 chlorides. By considering that the attack modes of HO° on aromatic heterocyclic compounds can be
285 summarized as hydroxylation, group substitution and H-abstraction, we suggested that myclobutanil
286 was firstly hydroxylated - as in a typical mechanism -, providing an intermediate with a higher
287 molecular weight than the parent compound (MW=304). This intermediate has been proposed to
288 follow two degradation routes. In the route A, it would undergo a second hydroxylation producing a
289 MW=221 Cl-containing C₁₀ intermediate with the elimination of an aliphatic compound, while the
290 route B would form a MW=192 Cl-free C₉ compound with the release of a Cl-phenol molecule. In
291 both cases, sequential hydroxylation steps would provoke the opening of the aromatic rings, with
292 consequently the formation of short-chain organic acids, further mineralized to CO₂. The detection in
293 the reaction media of chloride, nitrate and ammonium ions coming from the pesticide heteroatoms
294 corroborated this ring-opening and so the complete mineralization. Independently from the
295 degradation routes proposed, this evidenced that the photocatalytic degradation of myclobutanil did
296 not differ phenomenologically from the usual photo-oxidation of aromatic ring-pollutants *via*
297 different AOPs [37].

298 The ecotoxicological investigations with myclobutanil showed a total detoxification of the
299 solution single substance for daphnids already after 60 min of photocatalytic treatment. This is
300 evidenced by a significant increase of the 48 h-EC₅₀ value from 6 %TI to not measurable effects above
301 56 %TI. In the literature, 48 h-EC₅₀ values for myclobutanil were found to be dependent on its

302 individual enantiomers. However, for the rac-compound the value was calculated to be 9.24 mg/L,
303 which is approximatively 7.5 times higher than the value in the present study (which is 1.2 mg
304 myclobutanil/L). This, however, is not in a sharp contrast when also considering the 95% CI ranging
305 from 0 to 7.2 mg myclobutanil/L of the EC₅₀ values. In the study of Sun et al., there is unfortunately
306 no error provided for the EC₅₀ of myclobutanil [38]. However, the comparably wide confidence
307 interval (CI) in the present study let suggest that a statistically significant difference between both
308 EC₅₀ values may not be given.

309

310 **3.2. Degradation of glyphosate and myclobutanil pesticide mixture**

311 The influence of the co-presence of both glyphosate and myclobutanil in water on the treatment
312 performances was first screened using pesticide concentrations identical to those used for the single
313 pesticide degradation tests (*ie.* at a glyphosate and myclobutanil initial concentration of 25 mg/L and
314 20 mg/L, respectively, and the results are shown in Figure S3). The unusual TOC and myclobutanil
315 concentration profiles obtained - with a slight increase in TOC and a delayed myclobutanil removal
316 after an initial concentration plateau -, led us to further perform the study with a twice higher
317 myclobutanil initial concentration while maintaining unchanged that of glyphosate, in order to
318 highlight and to make this unusual behavior more visible, *ie* with a glyphosate and myclobutanil
319 initial concentration of 25 mg/L and 40 mg/L, respectively.

320 Figure 5 shows the evolution with time under irradiation of both the glyphosate and the
321 myclobutanil substrate removal rates in %, of the TOC, of the AMPA intermediate concentration and
322 of the chloride release in %. The evolution profile of the short chain acids, the N-compounds and of
323 the myclobutanil aromatic intermediates is shown in Figure S6-A and Figure S4-B, respectively. First,
324 it could be seen that glyphosate preferentially adsorbed on the TiO₂ surface during the dark
325 adsorption period, while no significant adsorption of myclobutanil was observed (Figure S1c). The
326 glyphosate adsorption was higher than in the case of the pure glyphosate solution (80% vs. 50%), as a

327 result of the less acidic pH of the solution (5.6 vs. 4.2), that increased the glyphosate dissociation and
328 consequently the concentration of the anionic form of glyphosate interacting with the positively-
329 charge surface of TiO₂. Glyphosate was first removed within 90 min of reaction, whereas the
330 oxidation of myclobutanil only took place once the complete glyphosate removal was reached. It
331 seems that the glyphosate adsorption onto the catalyst surface limits the oxidation of the co-present
332 pesticide, due to the surface saturation by the glyphosate compound after the adsorption
333 equilibrium, as confirmed by the pre-adsorption experiment in the dark. Furthermore, complete
334 mineralization of myclobutanil and complete removal TOC were achieved within 420 min and 900
335 min of reaction.

336 The detection of AMPA as reaction intermediate and the release of phosphate with a full closure
337 of the phosphorous mass balance, suggested that glyphosate is being degraded *via* a similar
338 mechanism as for the single pesticide. However, the kinetic rate constant of glyphosate depletion
339 was reduced from 0.096 to 0.027 min⁻¹ (Table 4), with a delayed on both the AMPA and the
340 phosphate evolution. By contrast, once the oxidation of myclobutanil has been initiated, no
341 significant difference was observed in terms of kinetic rate constant for the myclobutanil degradation
342 compared to that obtained with the pure substrate ($k' = 0.027 \text{ min}^{-1}$ vs. 0.021 min^{-1} for myclobutanil
343 alone), indicating that its depletion was not affected in terms of kinetics by the presence of the
344 phosphates and of the glyphosate degradation intermediates. The chloride balance was closed by the
345 release of chloride ions, indicating the absence of any residual organochloride species at the end of
346 the reaction. Also, it is worth noting that the TOC evolution displayed a *volcano*-profile in TOC values
347 at the beginning of the test, as in the case of the treatment of the single herbicide. The phosphorous
348 mass balance was closed in two steps: first, with an initial release of the 70% of stoichiometric
349 phosphates accompanied by the degradation of AMPA, followed by the subsequent release of the
350 remaining 30% of phosphates for longer reaction times ($\approx 600 \text{ min}$). Also, a second maximum was
351 observed at $\approx 650 \text{ min}$ in the TOC profile after the closure of the phosphorous balance, so that this
352 might also be attributed to the desorption of intermediates resulting from a N-C bond cleavage (the

353 experiment has been triplicated for validating the presence of this maximum, and the obtained
354 standard errors are reported on the TOC profile).

355 Indeed, the residual presence of N-C bond-containing sarcosine after 480 min and 540 min of
356 reaction was evidenced by LC MS/MS. The presence of intermediates from the myclobutanil
357 degradation might hinder the adsorption of this N-C bond-containing intermediate issued from the
358 glyphosate degradation, so that this volcano-profile was observed for longer treatment times, and
359 was not observed when glyphosate was treated as single pollutant. As far as myclobutanil
360 intermediates were concerned, the same metabolites were identified, indicating that the co-
361 presence of pesticides did not interfere in the myclobutanil oxidation routes (Figure S4-B).

362 For the mixture of myclobutanil and glyphosate (25:40 weight ratio), an interim but non-
363 statistically significant increase of toxicity for daphnia was observed after 180 min. In detail, the
364 initial 48 h-EC₅₀ value of 24 %TI decreased by approximately 20% down to 20 %TI (Table 3). This
365 toxicity increase may be related to the presence of reaction intermediates issued from the
366 glyphosate degradation, since an interim increase of toxicity was also observed during the case of the
367 single glyphosate treatment. We also cannot rule out the existence of a synergistic interaction effect
368 between the substrates and/or the reaction intermediates issued from the degradation of both
369 pesticides [39]. Hence, a treatment of 900 min was needed to decrease the toxicity until values
370 above calculable EC₅₀ values occurred. This is in good agreement with the complete mineralization of
371 both substrates at 900 min.

372

373 **3.3. Degradation of active substances within commercial formulations**

374 The degradation of the Roundup® solution was performed with an initial glyphosate
375 concentration of 25 mg/L and an initial TOC value of 20 mg/L, within which the glyphosate active
376 compound amounted only for 5.3 mg/L (Figure 1, Table 2). This extra-load of organic carbon coming

377 from the components contained in Roundup will be also oxidized unselectively. However, this extra-
378 load did not alter the glyphosate concentration profile, and only the duration necessary for achieving
379 the complete disappearance of glyphosate was extended to 100 min. Like in the case of glyphosate
380 alone, the *volcano-like* TOC profile observed at the beginning of the test could be attributed to the C-
381 N and C-P bond cleavage. It was therefore proposed that the mechanism followed the same pathway
382 and that the components contained in the Roundup did not interfere into the glyphosate
383 mineralization routes. However, the competitive adsorption on the catalyst surface of glyphosate
384 and its degradation intermediates with isopropylamine, the surfactants and their degradation by-
385 products impacted on the kinetic rate constant of glyphosate removal (reduced to $k' = 0,011 \text{ min}^{-1}$)
386 and on the intermediate evolution (AMPA, phosphate and aliphatic acids) that appeared for longer
387 reaction times. As a result, the reaction time necessary for achieving the complete TOC removal was
388 extended to 420 min, while the closure of the phosphorus balance confirmed that the total
389 mineralization was reached. Further, the presence of cations like Na^+ , K^+ or NH_4^+ (corroborated by
390 the conductivity measurements) and of anions like CO_3^{2-} in the matrix was detrimental for
391 photocatalysis due to the scavenging effect [5, 10].

392 For the untreated Roundup formulation, no toxicity for daphnia was observable, likely due to
393 a too low initial concentration of 12.5 mg/L (equal to 50 %TI, Table 3). This is in line with the
394 information from the product safety data sheet of Roundup®, which indicates a 48-h LC_{50} for Daphnia
395 as high as 930 mg/L [40].

396 A Systhane® solution with a myclobutanil concentration of 35 mg/L and a TOC value of 22
397 mg/L was treated (Figure 6B). Although the TOC measured was only related to the active compound,
398 the reaction time needed for reaching the complete myclobutanil conversion and mineralization was
399 slightly increased up to 240 min and 420 min, compared to 150 min and 240 min, respectively, in the
400 case of myclobutanil alone, with a decrease by half of the apparent kinetic rate constant for
401 myclobutanil removal down to $k'=0,013 \text{ min}^{-1}$. Compared to the oxidation of myclobutanil as single

402 substrate, a delay in the intermediate evolution was observed too (Figure S4-C), and the inorganic
403 chloride was only released after 120 min of irradiation (Figure 6B), 60 min delayed compared to the
404 single oxidation. The total depletion of the main organochloride compounds after 180min of reaction
405 (Figure S4C) was corroborated by the release of chloride ions that closed the chloride mass balance
406 after 420 min of treatment. This demonstrated that, although Kaolin was recently employed as
407 adsorbent for removing pollutants from water [41-43], it did not act as sorbent for storing chloride
408 ions issued from the myclobutanil degradation.

409 The delay of the intermediates evolution has been attributed to the presence of cations and
410 anions present in the commercial formulation (corroborated by the detection with ionic
411 chromatograph), which partially inhibited the process, but also to a screening effect resulting from
412 the presence of inorganic particles in suspension, which reduced the light penetration into the
413 solution and consequently was lowering the treatment efficiency. This hypothesis was supported by
414 the substantial increase in the rate of myclobutanil disappearance obtained when using a filtered
415 Systhane® solution (Figure S5). Surprisingly, only C8 and C9 metabolites were identified as reaction
416 intermediates among those detected when the reaction was performed with the synthetic ultrapure
417 water, whether myclobutanil was as single substrate or mixed with glyphosate (Figure S4). This
418 indicated that the degradation pathway was forced to go *via* the route B (C8) (Figure 4 route B)
419 rather than *via* the route A (C10) (Figure 4 route A). This suggested that the co-existence of the
420 cations and anions and of the inorganic oxide particles within the Systhane® formulation matrix could
421 affect the oxidation pathway and so drive selectively the mineralization process towards the
422 oxidation route B. Recently, Meephon et al. [44] observed during the study of the linuron
423 degradation with ZnO photocatalyst that changes in the adsorption alignment of linuron onto the
424 catalyst surface led to different degradation intermediates. In this work, the authors concluded that
425 the exposed surface of the photocatalyst was the key-factor driving the degradation pathway. In our
426 case, the co-presence of inorganic and ionic substances could alter the way myclobutanil adsorbs at
427 the surface and consequently provoke the formation of different intermediates during the process.

428 The ecotoxicity screening for the Systhane® formulation showed a successful reduction of the
429 toxicity of the solution already after 80 min of photocatalytic treatment (Table 3). Indeed, the 48-h
430 EC₅₀ value for the untreated product (40 %TI; 13.9 mg myclobutanil/L) increased to > 50 %TI after 80
431 min and 360 min of treatment.

432 Finally, the mixture of both commercially available items was treated and the results are
433 shown in Figure 6C and in Figures S6 and S7. The initial myclobutanil concentration was
434 approximatively half that of the single Systhane® tests, due to the highly viscous nature of the
435 commercial Systhane® paste that somehow slightly jeopardizes the initial concentration. This
436 explained the more visible initial adsorption of myclobutanil when compared to the single Systhane®
437 solution test. While the results showed that glyphosate was the first pesticide to be degraded within
438 120 min of test, a delay in both the myclobutanil and TOC reduction was observed, together with a
439 delay in the intermediate appearance, similarly to the above-reported cases. While both
440 phosphorous and chloride balances were fully closed by the release of phosphate and chloride ions,
441 respectively, it is worth noting that only the intermediates corresponding to the proposed
442 degradation route B have been observed, similarly to the case of the pesticide mix. Also, probably
443 due to the lower kinetic rates in the case of the complex matrix, the presence of sarcosine was
444 evidenced during the test (Figure S7). Interestingly, full mineralization was achieved faster than in
445 the case of the glyphosate and myclobutanil mixture, *ie.* 420 min vs. 900 min. This might possibly
446 result from a positive role of adsorbent played by the inorganic Kaolin additive from Systhane® that
447 might reduce the strong competitive adsorption occurring between the different carbonated molecules
448 observed in the case of the pesticide mix. The apparent kinetic rate constant for glyphosate
449 degradation was not affected by the co-presence of Systhane®, and although an additional drop of
450 the kinetic rate constant for the myclobutanil degradation was observed compared to Systhane®
451 (with $k' = 0,002 \text{ min}^{-1}$, Table 4), both the complete removal of the target pesticides and the reduction
452 in the acute toxicity with the treatment time were observed. This confirmed the viability of the
453 photocatalytic process to treat complex commercial formulation-containing wastewaters in the case

454 of glyphosate and myclobutanil pesticides.

455

456 **3.4. Evaluation of the matrix effect**

457 Figure 7 summarizes the influence of the water matrix on the evolution of both the glyphosate
458 and the myclobutanil pesticide concentration upon photocatalysis. The increase in the water matrix
459 complexity did not alter the overall glyphosate evolution profile, with the time required for removing
460 glyphosate being extended from 30 min to 120 min (Figure 7A). By contrast, in addition to the
461 increased time necessary for the elimination of myclobutanil from 150 min to 360 min, the co-
462 presence of glyphosate and of its additives in the Roundup® formulation strongly influenced the
463 overall myclobutanil evolution profile, as a result of the preferential adsorption of glyphosate on the
464 TiO₂ surface. Indeed, the co-presence of glyphosate – and to a lesser extent of the Roundup®
465 additives – caused a delay in the myclobutanil disappearance before a usual disappearance profile
466 was observed. It was worth noting that the additives from Systhane® had a less pronounced
467 influence on the myclobutanil removal duration than the glyphosate and the additives from
468 Roundup® had, probably due to their inorganic nature.

469 A duration of 240 min has been selected for evidencing the influence of the water matrix
470 complexity on the efficiency of the photocatalytic treatment in terms of TOC removal (X_{240}), since it
471 allowed the complete removal and mineralization of single pesticides (Figure 8). In the case of the
472 mixtures of pesticides, the X_{240} TOC removal efficiency strongly dropped down to 55% and 25% for
473 the 25:20 and 25:40 glyphosate:myclobutanil weight ratios, respectively, all the more pronounced as
474 the myclobutanil concentration increased. By contrast, a high TOC removal efficiency in the 65-85%
475 range was maintained in the case of the commercial formulations. Although the mineralization
476 efficiency was influenced by the presence of the additional organic components in the Roundup®
477 formulation – and in a lesser extent by that of the additional inorganic matter in the Systhane®
478 product, this suggested that the mineralization efficiency was more affected by the co-presence of

479 myclobutanil than by the presence of the inorganic additives or by that of the organic additives that
480 are more easily oxidized than myclobutanil.

481 Both pesticides and their corresponding commercial formulations differ strongly in terms of
482 chemical structure and composition, glyphosate being an aliphatic-type structure while myclobutanil
483 is mainly constituted by aromatic rings, and either organic or inorganic additives being used in the
484 commercial formulations. Table 4 shows that the apparent kinetic rate constants for the pesticide
485 degradation were highly impacted by the presence of the matrix components, – although in a very
486 different way according to the substrate, the degradation mechanism for glyphosate being notably
487 mediated by the adsorption onto the surface catalyst – ; an overall drastic reduction was observed
488 from 0.096 min^{-1} and 0.021 min^{-1} for the single glyphosate and myclobutanil degradation,
489 respectively, to 0.011 min^{-1} and 0.002 min^{-1} for the commercial formulation mixture. However, for
490 both pesticides, the degradation kinetic rate constant maintained in the commercial Roundup® and
491 Systhane® formulation mix about 10% of the corresponding value obtained in the case of the single
492 pesticide.

493 Interestingly, the ecotoxicity of the untreated Systhane® x Roundup® mixture was higher
494 than that of the single substances, being *eg.* approximately 3-fold more toxic for daphnids than the
495 untreated Systhane® solution (Table 3). As the Roundup® solution solely did not show any effects on
496 daphnids, this indicated the occurrence of a synergistic effect. The photocatalytic treatment of the
497 commercial formulation mixture statistically significantly reduced the water toxicity already after 60
498 min of process, and by approximately 50% after 360 min of treatment (25 %TI vs. 54 %TI), although
499 a total degradation and mineralization of the myclobutanil and glyphosate active substances in the
500 Systhane® and Roundup® products was analytically detected (Figure 7). This might result from the
501 existence of a synergistic interaction effect involving species remaining in the treated water as trace
502 level.

503

504 4. CONCLUSION

505

506 Independently of the water matrix complexity, both glyphosate and myclobutanil pesticides
507 were degraded using Aeroxide TiO₂-P25 as reference photocatalyst under UV-A irradiation, with a
508 complete mineralization yield into CO₂, chloride and phosphate ions. The glyphosate degradation has
509 been proposed to occur *via* both AMPA and sarcosine pathways with an unusual volcano-like profile
510 for the TOC evolution resulting from the degradation pathway, while the photocatalytic degradation
511 of myclobutanil did not phenomenologically differ from the usual photo-oxidation of aromatic ring-
512 pollutants by AOPs. The overall pesticide evolution profiles were not affected by the water matrix
513 complexity, except that the time necessary for the complete removal of both pesticides increased
514 with increasing the matrix complexity. We showed that the myclobutanil evolution profile was
515 strongly influenced by the co-presence of glyphosate – and to lesser extent of its additives in the
516 Roundup® formulation –, as a result of the preferential glyphosate adsorption on the TiO₂ surface
517 that delayed the myclobutanil disappearance. By contrast, we provided further evidence that the
518 inorganic additives from Systhane® had a lower influence on the myclobutanil removal duration and
519 on the TOC removal efficiency when compared to that of the glyphosate/Roundup® products,
520 although they impacted on its degradation route.

521 However, although the apparent kinetic rate constants for glyphosate and myclobutanil
522 degradation and the mineralization efficiency were globally reduced with the increase in the water
523 matrix complexity, complete mineralization was achieved *via* photocatalysis, with a full closure of the
524 phosphorus and chlorine heteroatom balance as phosphate and chloride ions even in the case of the
525 commercial formulation mix, for which a significant decrease in the acute toxicity of the water for
526 daphnids was consequently obtained.

527 Works are ongoing for studying the reaction pathway and the influence of the aqueous
528 matrix complexity in the degradation of both pesticides under simulated solar light using visible-light
529 responsive photocatalysts, and for treating real wastewater in field experiments using immobilized
530 photocatalysts for demonstrating further the viability of the photocatalysis approach and increasing
531 the practical significance of the work.

532

533 **Acknowledgements.**

534 The authors want to thank the European Fund for regional development (EFRE/FEDER) for the
535 financial support of the PHOTOPUR project which is performed within the framework of Interreg V
536 and the Sciences Offensive.

537

538

539 **REFERENCES**

- 540 [1] I.C. M'Bra, P. García-Muñoz, P. Drogui, N. Keller, A. Trokourey, D. Robert, Heterogeneous
541 photodegradation of Pyrimethanil and its commercial formulation with TiO₂ immobilized on SiC
542 foams, *J. Photochem. Photobiol. A Chem.* 368 (2019) 1-6.
- 543 [2] N. De Castro-Català, I. Muñoz, L. Armendáriz, B. Campos, D. Barceló, J. López-Doval, S. Pérez, M.
544 Petrovic, Y. Picó, J.L. Riera, Invertebrate community responses to emerging water pollutants in
545 Iberian river basins, *Science of The Total Environment.* 503-504 (2015) 142-150.
- 546 [3] I. Oller, S. Malato, J.A. Sánchez-Pérez, Combination of Advanced Oxidation Processes and
547 biological treatments for wastewater decontamination—A review, *Science of The Total Environment.*
548 409 (2011) 4141-4166.
- 549 [4] R. Münze, C. Hannemann, P. Orlinskiy, R. Gunold, A. Paschke, K. Foit, J. Becker, O. Kaske, E.
550 Paulsson, M. Peterson, H. Jernstedt, J. Kreuger, G. Schüürmann, M. Liess, Pesticides from wastewater
551 treatment plant effluents affect invertebrate communities, *Science of The Total Environment.* 599-
552 600 (2017) 387-399.
- 553 [5] S. Malato, P. Fernández-Ibáñez, M.I. Maldonado, J. Blanco, W. Gernjak, Decontamination and
554 disinfection of water by solar photocatalysis: Recent overview and trends, *Catalysis Today.* 147
555 (2009) 1-59.
- 556 [6] S. Esplugas, J. Giménez, S. Contreras, E. Pascual, M. Rodríguez, Comparison of different advanced
557 oxidation processes for phenol degradation, *Water Research.* 36 (2002) 1034-1042.
- 558 [7] S. Malato, J. Blanco, P. Fernández-Ibáñez, J. Calzadillas, Treatment of 2,4-Dichlorophenol by
559 Solar Photocatalysis: Comparison of Coupled Photocatalytic-Active Carbon vs. Active Carbon, *Journal*
560 *of Solar Energy Engineering.* 123 (2000) 138-142.

- 561 [8] A. Kushniarou, I. Garrido, J. Fenoll, N. Vela, P. Flores, G. Navarro, P. Hellín, S. Navarro, Solar
562 photocatalytic reclamation of agro-waste water polluted with twelve pesticides for agricultural
563 reuse, *Chemosphere*. 214 (2019) 839-845.
- 564 [9] C. Berberidou, V. Kitsiou, E. Kazala, D.A. Lambropoulou, A. Kouras, C.I. Kosma, T.A. Albanis, I.
565 Poullos, Study of the decomposition and detoxification of the herbicide bentazon by heterogeneous
566 photocatalysis: Kinetics, intermediates and transformation pathways, *Appl. Catal. B Environ.* 200
567 (2017) 150-163.
- 568 [10] J. Carbajo, P. García-Muñoz, A. Tolosana-Moranchel, M. Faraldos, A. Bahamonde, Effect of water
569 composition on the photocatalytic removal of pesticides with different TiO₂ catalysts, *Environmental
570 Science and Pollution Research* (2014).
- 571 [11] R. Vicente, J. Soler, A. Arques, A.M. Amat, Z. Frontistis, N. Xekoukoulotakis, D. Mantzavinos,
572 Comparison of different TiO₂ samples as photocatalyst for the degradation of a mixture of four
573 commercial pesticides, *J. Chem. Technol. Biotechnol.* 89 (2014) 1259-1264.
- 574 [12] A.L. Tasca, M. Puccini, A. Fletcher, Terbutylazine and desethylterbutylazine: Recent
575 occurrence, mobility and removal techniques, *Chemosphere*. 202 (2018) 94-104.
- 576 [13] A. García-Ripoll, A. Arques, R. Vicente, A. Domenech, A.M. Amat, Treatment of aqueous
577 solutions containing four commercial pesticides by means of TiO₂ solar photocatalysis, *J Sol Energy
578 Eng Trans ASME*. 130 (2008) 0410111-0410115.
- 579 [14] F. Seitz, R.R. Rosenfeldt, M. Müller, S. Lüderwald, R. Schulz, M. Bundschuh, Quantity and quality
580 of natural organic matter influence the ecotoxicity of titanium dioxide nanoparticles, *Nanotoxicology*.
581 10 (2016) 1415-1421.
- 582 [15] M. Peschka, Trends in pesticide transport into the River Rhine, *Handbook of Environmental
583 Chemistry, Volume 5: Water Pollution*. 5 (2006) 155-175.
- 584 [16] J.C. Niemeyer, F.B. de Santo, N. Guerra, A.M. Ricardo Filho, T.M. Pech, Do recommended doses
585 of glyphosate-based herbicides affect soil invertebrates? Field and laboratory screening tests to risk
586 assessment, *Chemosphere*. 198 (2018) 154-160.
- 587 [17] V.S. Andrade, M.F. Gutierrez, N.I. Fantão, A.M. Gagneten, Shifts in Zooplankton Behavior
588 Caused by a Mixture of Pesticides, *Water, Air, & Soil Pollution*. 229 (2018) 107.
- 589 [18] Z. Chen, G. Ying, Occurrence, fate and ecological risk of five typical azole fungicides as
590 therapeutic and personal care products in the environment: A review, *Environment International*. 84
591 (2015) 142-153.
- 592 [19] P. Westlund, V. Yargeau, Investigation of the presence and endocrine activities of pesticides
593 found in wastewater effluent using yeast-based bioassays, *Sci. Total Environ.* 607-608 (2017) 744-
594 751.
- 595 [20] H.T. Vu, M.J. Keough, S.M. Long, V.J. Pettigrove, Toxicological effects of fungicide mixtures on
596 the amphipod *Austrochiltonia subtenuis*, *Environ. Toxicol. Chem.* 36 (2017) 2651-2659.
- 597 [21] A. Kähler, S. Hellweg, B.I. Escher, K. Hungerbühler, Organic Pollutant Removal versus Toxicity
598 Reduction in Industrial Wastewater Treatment: The Example of Wastewater from Fluorescent
599 Whitening Agent Production, *Environ. Sci. Technol.* 40 (2006) 3395-3401.
- 600 [22] J. Liang, X. Ning, M. Kong, D. Liu, G. Wang, H. Cai, J. Sun, Y. Zhang, X. Lu, Y. Yuan, Elimination and
601 ecotoxicity evaluation of phthalic acid esters from textile-dyeing wastewater, *Environmental
602 Pollution*. 231 (2017) 115-122.
- 603 [23] S.D. Supowit, A.M. Sadaria, E.J. Reyes, R.U. Halden, Mass Balance of Fipronil and Total Toxicity of
604 Fipronil-Related Compounds in Process Streams during Conventional Wastewater and Wetland
605 Treatment, *Environ. Sci. Technol.* 50 (2016) 1519-1526.

606 [24] M.R. Assalin, S.G. De Moraes, S.C.N. Queiroz, V.L. Ferracini, N. Duran, Studies on degradation of
607 glyphosate by several oxidative chemical processes: Ozonation, photolysis and heterogeneous
608 photocatalysis, *Journal of Environmental Science and Health, Part B*. 45 (2009) 89-94.

609 [25] S. Chen, Y. Liu, Study on the photocatalytic degradation of glyphosate by TiO₂ photocatalyst,
610 *Chemosphere*. 67 (2007) 1010-1017.

611 [26] G.R.M. Echavia, F. Matzusawa, N. Negishi, Photocatalytic degradation of organophosphate and
612 phosphonoglycine pesticides using TiO₂ immobilized on silica gel, *Chemosphere*. 76 (2009) 595-600.

613 [27] T. Janin, V. Goetz, S. Brosillon, G. Plantard, Solar photocatalytic mineralization of 2,4-
614 dichlorophenol and mixtures of pesticides: Kinetic model of mineralization, *Solar Energy*. 87 (2013)
615 127-135.

616 [28] J. Fenoll, I. Garrido, M. Pastor-Belda, N. Campillo, P. Viñas, M.J. Yañez, N. Vela, S. Navarro, Solar
617 detoxification of water polluted with fungicide residues using ZnO-coated magnetic particles,
618 *Chemical Engineering Journal*. 330 (2017) 71-81.

619 [29] OECD, Test No. 202: Daphnia sp. Acute Immobilisation Test (2004).

620 [30] T.T.T. Dang, S.T.T. Le, D. Channei, W. Khanitchaidecha, A. Nakaruk, Photodegradation
621 mechanisms of phenol in the photocatalytic process, *Res Chem Intermed*. 42 (2016) 5961-5974.

622 [31] M. Rani, U. Shanker, Photocatalytic degradation of toxic phenols from water using bimetallic
623 metal oxide nanostructures, *Colloids Surf. A Physicochem. Eng. Asp.* 553 (2018) 546-561.

624 [32] P. García-Muñoz, G. Pliego, J.A. Zazo, M. Munoz, Z.M. De Pedro, A. Bahamonde, J.A. Casas,
625 Treatment of hospital wastewater through the CWPO-Photoassisted process catalyzed by ilmenite, *J.*
626 *Environ. Chem. Eng.* 5 (2017) 4337-4343.

627 [33] D.P. Jaisi, H. Li, A.F. Wallace, P. Paudel, M. Sun, A. Balakrishna, R.N. Lerch, Mechanisms of Bond
628 Cleavage during Manganese Oxide and UV Degradation of Glyphosate: Results from Phosphate
629 Oxygen Isotopes and Molecular Simulations, *J. Agric. Food Chem.* 64 (2016) 8474-8482.

630 [34] M. Barreto-Rodrigues, J. Silveira, P. García-Muñoz, J.J. Rodriguez, Dechlorination and oxidative
631 degradation of 4-chlorophenol with nanostructured iron-silver alginate beads, *J. Environ. Chem. Eng.*
632 5 (2017) 838-842.

633 [35] S. Komtchou, A. Dirany, P. Drogui, N. Delegan, M.A. El Khakani, D. Robert, P. Lafrance,
634 Degradation of atrazine in aqueous solution with electrophotocatalytic process using TiO₂-x
635 photoanode, *Chemosphere*. 157 (2016) 79-88.

636 [36] W.W. Lai, H.H. Lin, A.Y. Lin, TiO₂ photocatalytic degradation and transformation of
637 oxazaphosphorine drugs in an aqueous environment, *Journal of Hazardous Materials*. 287 (2015)
638 133-141.

639 [37] M. Munoz, F.J. Mora, Z.M. de Pedro, S. Alvarez-Torrellas, J.A. Casas, J.J. Rodriguez, Application of
640 CWPO to the treatment of pharmaceutical emerging pollutants in different water matrices with a
641 ferromagnetic catalyst, *J. Hazard. Mater.* 331 (2017) 45-54.

642 [38] M. Sun, L. Donghui, Q. Xinxu, Z. Qian, S. Zhigang, W. Peng, Z. Zhiqiang, Acute Toxicity, Bioactivity,
643 and Enantioselective Behavior with Tissue Distribution in Rabbits of Myclobutanil Enantiomers,
644 *Chirality*. 26 (2014) 784-789.

645 [39] S. Loureiro, C. Svendsen, A.L.G. Ferreira, C. Pinheiro, F. Ribeiro, A.M.V.M. Soares, Toxicity of
646 three binary mixtures to *Daphnia magna*: Comparing chemical modes of action and deviations from
647 conceptual models, *Environmental Toxicology and Chemistry*. 29 (2010) 1716-1726.

648 [40] J. Schuette, Environmental fate of Glyphosate.
649 Environmental Monitoring & Pest Management Department of Pesticide Regulation Sacramento, CA
650 95824-562 (1998).

- 651 [41] H.S. Vardikar, B.A. Bhanvase, A.P. Rathod, S.H. Sonawane, Sonochemical synthesis,
652 characterization and sorption study of Kaolin-Chitosan-TiO₂ ternary nanocomposite: Advantage over
653 conventional method, *Mater. Chem. Phys.* 217 (2018) 457-467.
- 654 [42] M.W. Amer, A.M. Awwad, Removal of As(V) from aqueous solution by adsorption onto
655 nanocrystalline kaolinite: Equilibrium and thermodynamic aspects of adsorption, *Environ.*
656 *Nanotechnol. Monit. Manag.* 9 (2018) 37-41.
- 657 [43] H. Xu, J. Liu, P. Chen, G. Shao, B. Fan, H. Wang, D. Chen, H. Lu, R. Zhang, Preparation of Magnetic
658 Kaolinite Nanotubes for the Removal of Methylene Blue from Aqueous Solution, *J. Inorg. Organomet.*
659 *Polym. Mater.* 28 (2018) 790-799.
- 660 [44] S. Meephon, T. Rungrotmongkol, N. Kaiyawet, S. Puttamat, V. Pavarajarn, Surface-Dependence
661 of Adsorption and Its Influence on Heterogeneous Photocatalytic Reaction: A Case of Photocatalytic
662 Degradation of Linuron on Zinc Oxide, *Catalysis Letters.* 148 (2018) 873-881.
- 663 [45] Datasheet, SYSTHANE™ 40WP Fungicide datasheet. 2018.
- 664 [46] J.P. Giesy, S. Dobson, K.R. Solomon, Ecotoxicological risk assessment for Roundup® herbicide,
665 *Rev. Environ. Contam. Toxicol.* 167 (2000) 35-120.
- 666

Figure 1

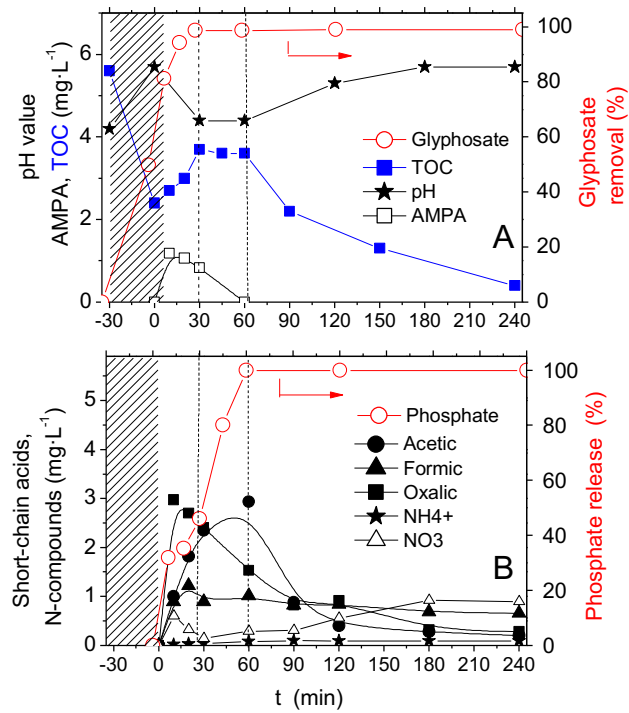


Figure 1. Evolution with time under irradiation of (A) glyphosate ($C_0 = 25 \text{ mg/L}$, $\text{TOC}_0 = 5.3 \text{ mg/L}$) removal in %, TOC and pH, (B) Short-chain acids, nitrate, ammonium and phosphate release in %. The dashed area corresponds to the dark equilibrium period.

Figure 2

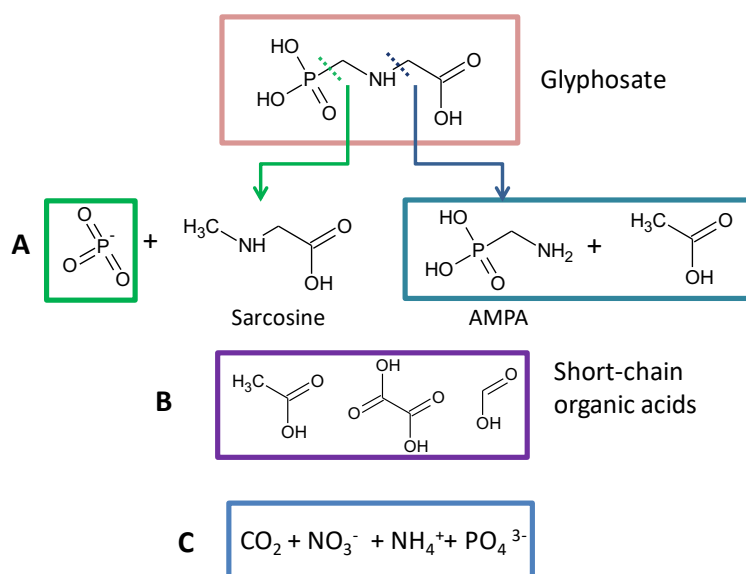


Figure 2. Proposed degradation route for the removal of glyphosate by photocatalysis based on both AMPA and sarcosine pathways with C-N and C-P cleavage, respectively, according to the reaction intermediates and final products detected. The detected molecules are framed. **A-left:** phosphate and sarcosine intermediate; **A-right:** AMPA and acetic acid; **B:** acetic, oxalic and formic acids; **C:** carbon dioxide and ions.

Figure 3

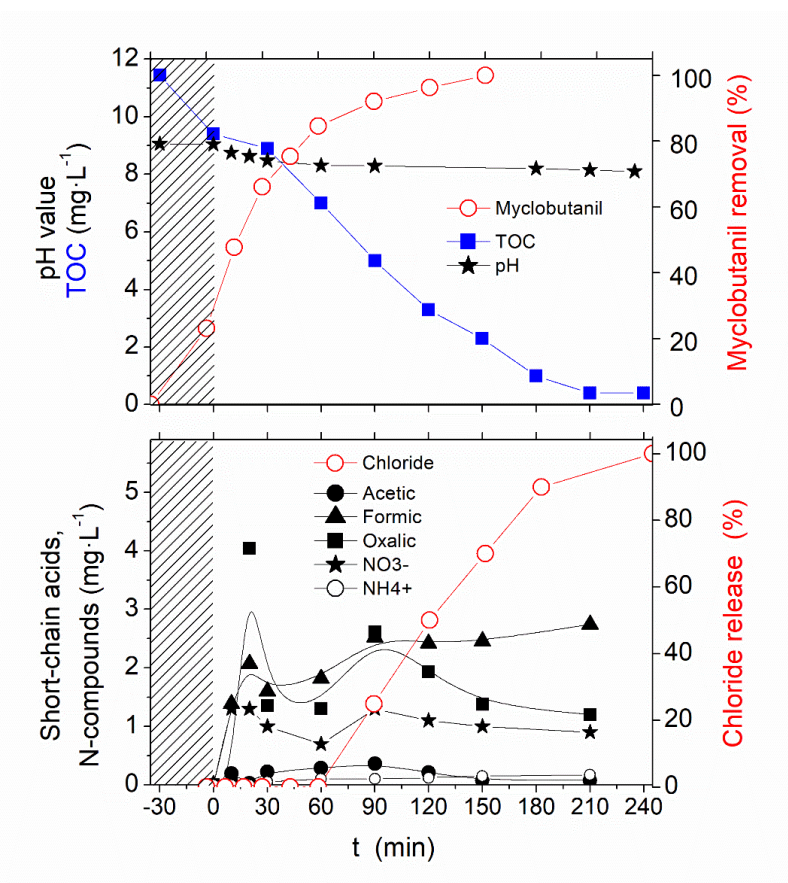


Figure 3. Evolution with time under irradiation of (A) myclobutanil ($C_0= 20 \text{ mg/L}$, $\text{TOC}_0= 12.5 \text{ mg/L}$) removal in %, TOC and pH, (B) Short-chain acids, aliphatic acids, nitrate, ammonium and chloride release in %. The dashed area corresponds to the dark equilibrium period.

Figure 4

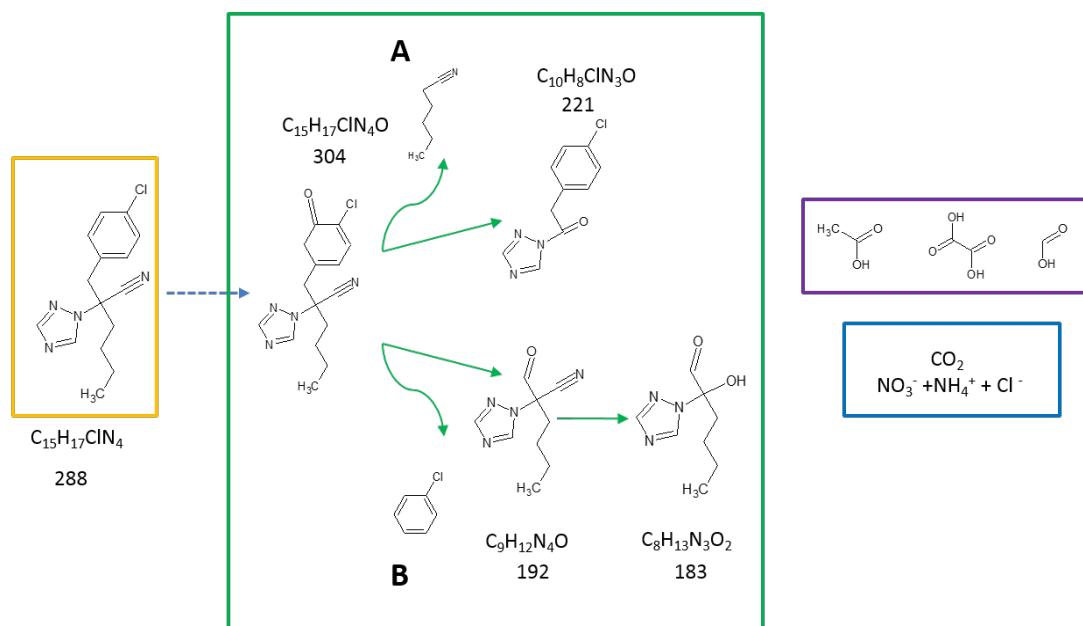


Figure 4. Proposed degradation route for the removal of myclobutanil by photocatalysis, according to the reaction intermediates and final products detected. The detected molecules are framed.

Figure 5

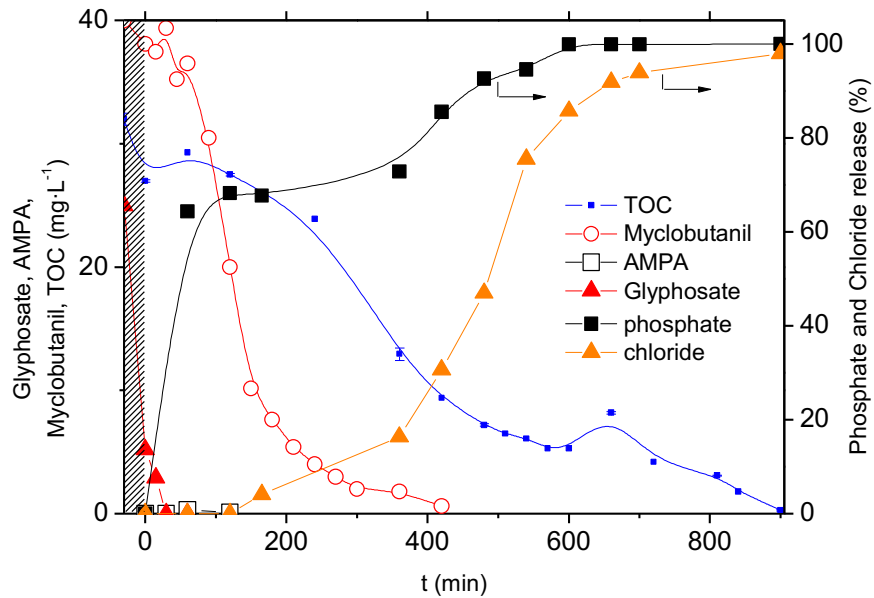
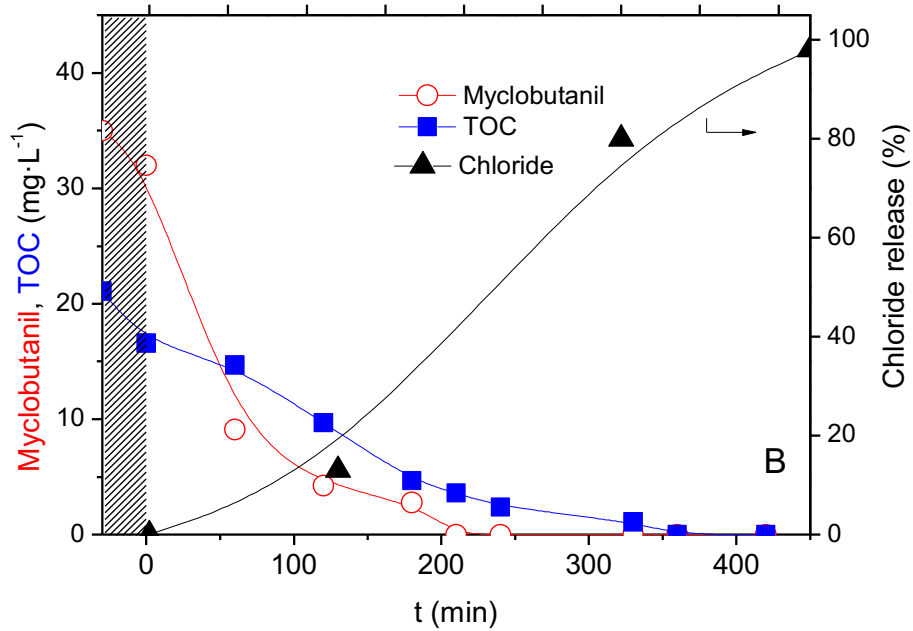
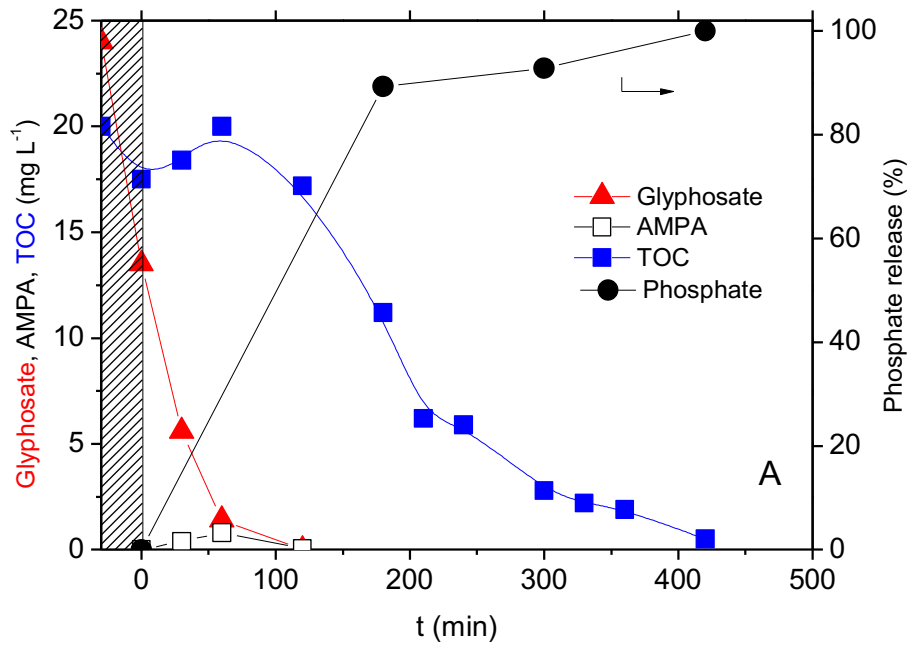


Figure 5. Evolution with time under irradiation of glyphosate ($C_0 = 25$ mg/L, $TOC_0 = 5.3$ mg/L), myclobutanil ($C_0 = 40$ mg/L, $TOC_0 = 24.9$ mg/L), AMPA and TOC concentrations, and of both phosphate and chloride release in % during the simultaneous removal of both glyphosate and myclobutanil pesticides with a 25:40 weight ratio. The dashed area corresponds to the dark equilibrium period. The experiment has been triplicated for validating the presence of a maximum in the TOC profile at ≈ 650 min, and the obtained standard errors are reported on the TOC profile.

Figure 6



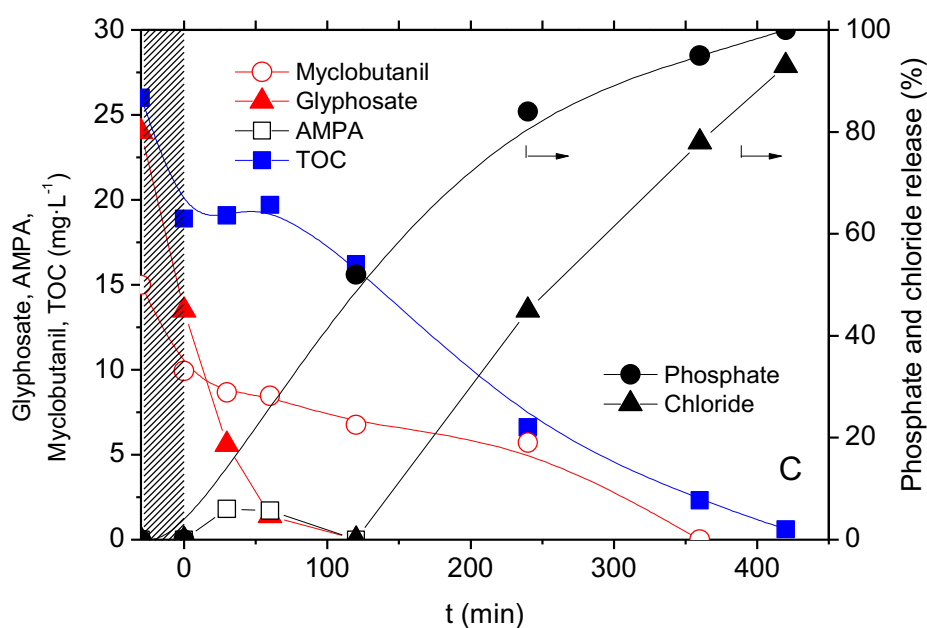


Figure 6. Photocatalytic treatment of commercial pesticide solutions: (A) Roundup® (containing glyphosate), (B) Systhane® (containing myclobutanil), and (C) Roundup® and Systhane® mix. The dashed area corresponds to the dark equilibrium period. A lower initial myclobutanil concentration (15 mg/L) was used in the case of the product mix, as a result of the highly viscous nature of the commercial Systhane® paste that somehow jeopardizes the initial myclobutanil concentration of the pesticide mix solution.

Figure 7

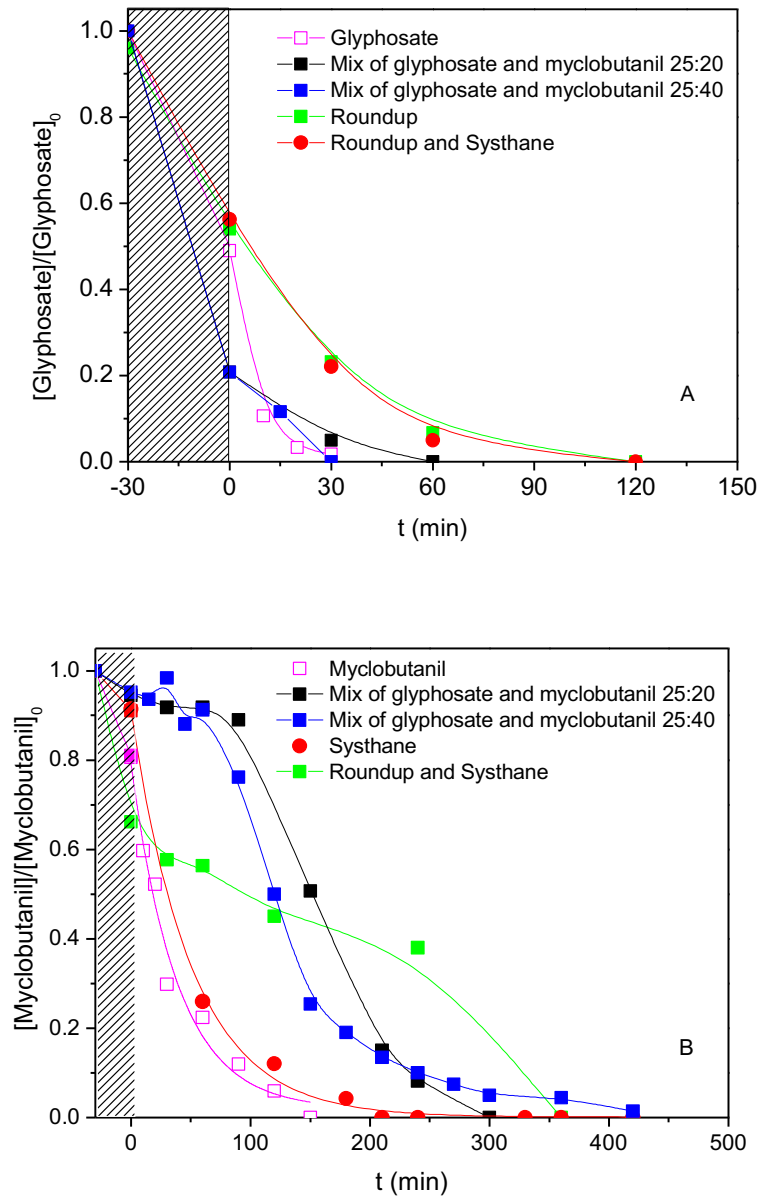


Figure 7. Influence of the water matrix complexity on the evolution with time under irradiation of (A) glyphosate and (B) myclobutanil concentrations. The dashed area corresponds to the dark equilibrium period. The mix of commercial formulations is obtained with a volume ratio of Roundup® to Systhane® of 1:1.

Figure 8

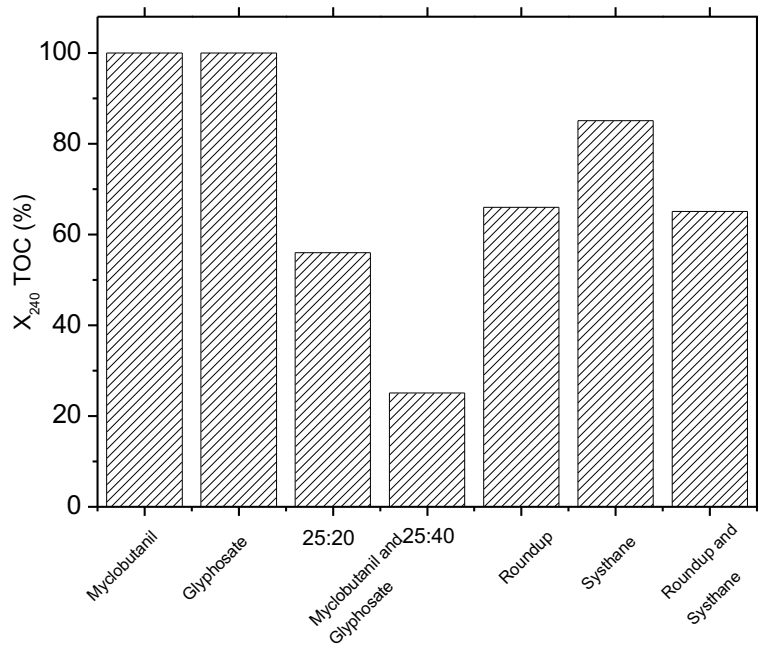


Figure 8. TOC conversion for the glyphosate and myclobutanil degradation in different water matrices.

Table 1. Main components of the Roundup®-720 and Systhane®-200 commercial formulations as identified from the manufacturer's datasheets and the literature [45, 46] .

Roundup®-720		Systhane®-200	
Component	Mass percentage (%)	Component	Mass percentage (%)
Glyphosate	41	Myclobutanil	40
Isopropylamine	44	Kaolin	<40
Surfactants	15	Calcium polysilicate	<5
		Silica	<1
		Titanium dioxide	1.1

Table 2. Physico-chemical parameters of the ready-to-use diluted commercial formulations.

	Roundup®	Systhane®
[Active ingredient] (mg/L) ^a	25	35
Total TOC (mg/L) ^b	20	22
TOC _{active compound} (mg/L) ^c	5,3	22
pH ₀	5,5	6,3
IC (mg/L) ^b	3,2	1,5
Conductivity (µS/cm)	145	32

^a measured concentration of the active ingredients

^b obtained by TOC analysis

^c TOC value corresponding to the measured concentration of the active compounds

Table 3: 48-h EC₅₀ values and respective lower and upper 95% Confidence Intervals (LCI, UCI) of the test items for *Daphnia magna* at different times of the photocatalytic treatment, expressed in percentage of test item volume within the test solution (= %TI).

Samples	t (min)	48 h-EC ₅₀ expressed in %TI [expressed in mg/L]*	95% LCI	95% UCI
<i>Glyphosate</i>	Initial	> 50 [> 25.0]	NA	NA
	60	55	38	72
	120	41	NA	NA
	240	>50	NA	NA
<i>Myclobutanil</i>	Initial	6 [1.2]	0	36
	60	>56	NA	NA
	150	>56	NA	NA
	240	>56	NA	NA
<i>Glyphosate x Myclobutanil</i>	Initial	24	12	36
	180	20	16	23
	900	NA	NA	NA
<i>Roundup</i>	Initial	>50 [> 12.5]	NA	NA
	80	>50	NA	NA
	300	>50	NA	NA
<i>Sythane</i>	Initial	40 [13.9]	25	55
	80	>50	NA	NA
	360	>50	NA	NA
<i>Roundup x Sythane</i>	Initial	25	22	27
	60	38	34	42
	180	42	34	50
	360	54	47	61

NA: mathematically not assessable

*: in square brackets, the EC₅₀ values in mg/L based on the nominal concentration are given. This is only possible for single substances and initial solutions.

Table 4. Influence of the water matrix complexity on the apparent kinetic rate constant for glyphosate and myclobutanil degradation

	$k'_{\text{Glyphosate}}$ (min^{-1})/ R^2	$k'_{\text{Myclobutanil}}$ (min^{-1})/ R^2
Glyphosate	0.096/0.99	-
Myclobutanil	-	0.021/0.99
Glyphosate and myclobutanil (25:40)	0.027/0.99	0.027/0.99
Roundup®	0.011/0.99	-
Sythane®	-	0.013/0.99
Roundup® and Sythane® mix	0.011/0.98	0.002/0.99